LETTER **Communicated by Terrence Sejnowski**

A Compartmental Model of Linear Resonance and Signal Transfer in Dendrites

Alan Schoen
alan.schoen@mail.mcgill.ca
Department of Physiology, McGill University, Montreal, Quebec H3G 1Y6, Canada

Ali Salehiomran
ali.salehiomran@mail.mcgill.ca
Department of Electrical and Computer Engineering, McGill University, Montreal, Quebec H3A 0E9, Canada

Matthew E. Larkum
larkumma@hu-berlin.de
Neurocure Cluster of Excellence, Department of Biology, Humboldt University, 10117, Berlin, Germany

Erik P. Cook
erik.cook@mcgill.ca
Department of Physiology, McGill University, Montreal, Quebec H3G 1Y6, Canada

Dendrites carry signals between synapses and the soma and play a central role in neural computation. Although they contain many nonlinear ion channels, their signal-transfer properties are linear under some experimental conditions. In experiments with continuous-time inputs, a resonant linear two-port model has been shown to provide a near-perfect fit to the dendrite-to-soma input-output relationship. In this study, we focused on this linear aspect of signal transfer using impedance functions that replace biophysical channel models in order to describe the electrical properties of the dendritic membrane. The membrane impedance model of dendrites preserves the accuracy of the two-port model with minimal computational complexity. Using this approach, we demonstrate two membrane impedance profiles of dendrites that reproduced the experimentally observed two-port results. These impedance profiles demonstrate that the two-port results are compatible with different computational schemes. In addition, our model highlights how dendritic resonance can minimize the location-dependent attenuation of signals at the resonant frequency. Thus, in this model, dendrites function as linear-resonant filters that carry signals between nonlinear computational units.

1 Introduction

Dendrites make up the majority of the surface area in neurons, and their signal processing properties determine how neurons integrate synaptic inputs. Accumulating experimental evidence shows that the voltage-dependent mechanisms of dendrites support a range of linear and nonlinear processing. For example, nonlinearities are prevalent in clusters of locally active synapses (Polsky, Mel, & Schiller, 2004; Gasparini, Migliore, & Magee, 2004; Larkum, Nevian, Sandler, Polsky, & Schiller, 2009; Spruston, 2008). However, linear processing has been reported in response to spatially diffuse synaptic inputs (Cash & Yuste, 1999; Polsky et al., 2004; Nevian, Larkum, Polsky, & Schiller, 2007; Jia, Rochefort, Chen, & Konnerth, 2010), dendritic current injections (Berger, Larkum, & Lüscher, 2001), and continuous-time current injections (Ulrich, 2002; Cook, Guest, Liang, Masse, & Colbert, 2007; Hu, Vervaeke, Graham, & Storm, 2009; Narayanan & Johnston, 2007).

The high degree of linear dendritic processing under continuous-time dendritic current injection has been particularly notable. These experiments avoided the influence of synaptic nonlinearities by injecting current directly into the dendritic membrane. Thus, they provided a clear picture of one part of the computational system in a neuron: electrical transmission across dendrites. The results are surprisingly consistent, with each experiment revealing a bandpass filter with resonance in the 1–10 Hz range. Our goal was to explore how the linearity and resonance of the soma-to-dendrite transfer function constrained a functional model of dendritic signal transfer.

In this study, we first provide a background summary of the linear dendritic properties revealed by these recent experiments. For our modeling results, we next demonstrate that linear-resonant signal transfer also occurs in a biophysically realistic model of a CA1 hippocampal neuron. We then derive an accurate, computationally efficient, compartmental model of a neuron that collapses the voltage- and time-dependent membrane properties of each compartment into a single membrane transfer impedance. Finally, we present two examples of linear models of dendrites that are consistent with the experimental signal-transfer observations.

2 Background: The Frequency Response of Dendrites

Neurons are complex systems with many interacting components. This study focuses on one part of the larger picture: dendrites as electrical conduits. Dendrites connect different parts of a neuron, and electrical signals travel over long stretches of dendritic membrane. We deliberately exclude axosomatic excitation and interactions between synapses to focus on dendritic signal transfer.

Several recent studies have directly measured the input-output and frequency response of dendrites using continuous-time current injection (Ulrich, 2002; Cook, Guest et al., 2007; Hu, Vervaeke, Graham, & Storm,

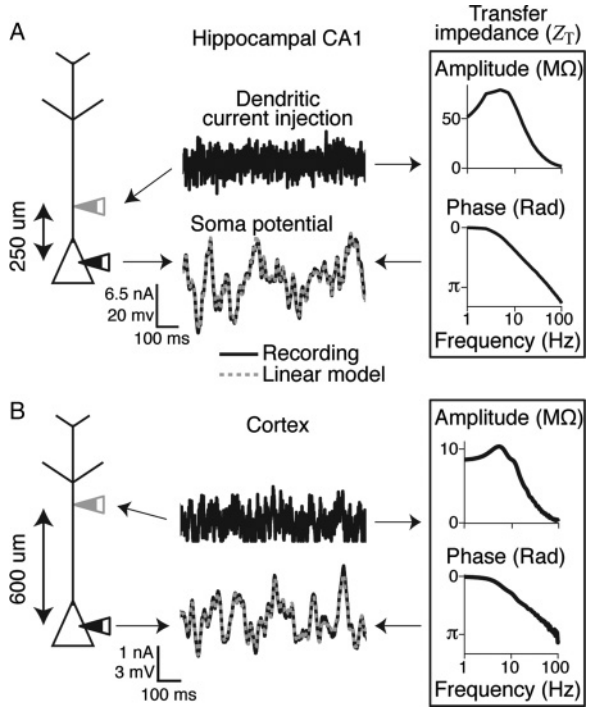

Figure 1: Frequency response of the dendrite-to-soma input-output response. Two example experiments are shown for a hippocampal CA1 pyramidal neuron (A), and cortical pyramidal neuron (B). Continuous broadband random current was injected on the apical trunk (gray electrode) and measured at the soma (black electrode). Short segments of injected current (top) and recorded soma potential (black, bottom) are shown. Each experiment was fit with a linear model, and the linear prediction (dashed gray) is superimposed on the soma potential. The linear model consisted of a transfer impedance Z_T with an amplitude and phase component. For details of the data collection and model fitting, see Cook, Guest et al. (2007) and Larkum et al. (2009).

2009; Narayanan & Johnston, 2007). Time-varying current injection is intended to mimic the effect of simultaneous input from many synapses. These studies used dual-patch clamp electrodes applied simultaneously to the dendrites and soma of either hippocampal or cortical pyramidal neurons. In the simplest version of these experiments, time-varying current (either white noise or a frequency chirp) was injected into the main apical dendritic trunk, and voltage was measured in the soma. Figures 1A and 1B illustrate this paradigm using a white noise current input applied to hippocampal and cortical neurons, respectively. From the injected dendritic

current and somatic voltage recording, systems identification was used to estimate the linear transfer function (referred to as the transfer impedance or Z_T) that best accounted for the input-output relationship.

These studies produced two interesting findings about dendritic transmission of time-varying signals: linearity and resonance. First, for all practical purposes, Z_T fully accounted for the dendrite-to-soma input-output relationship by predicting up to 98% of the variance of the soma voltage (Cook, Guest et al., 2007). Our two example neurons in Figure 1 illustrate this linearity by showing a short segment of the somatic voltage predicted by Z_T (gray dashed line) plotted with the actual recorded membrane potential (solid black line). Together with other observations of linearity (Berger, Larkum, & Lüscher, 2001), these results suggest that under continuous time-varying current injections, the main dendritic trunk is a linear band pass filter.

That a linear transfer impedance captured the signal-transfer capabilities is remarkable since dendrites have a full complement of nonlinear voltage-dependent channels. Cook, Guest et al. (2007) found that linearity was preserved even when the injected current was strong enough to evoke action potentials as long as the spikes were removed from the somatic voltage trace before estimating the transfer impedance. In Figure 1A, for example, 1.2% of the voltage trace was composed of action potentials in the hippocampal data shown. Hu et al. (2009) also confirmed that dendrites obey the symmetric property of linear two-port systems; the dendrite-to-soma transfer impedance and soma-to-dendrite transfer impedance were found to be the same. In addition, it has been suggested that interactions between nonlinear channels can produce linear behavior under some conditions (Morel & Levy, 2009).

The second notable outcome of these experiments is that the input-output relationship has a resonant frequency response around 1 to 10 Hz (Ulrich, 2002; Cook, Guest et al., 2007; Hu et al., 2009; Narayanan & Johnston, 2007). This resonance is illustrated in Z_T for our two example neurons in Figure 1. Note that the cortical pyramidal neuron's resonance band is slightly narrower than that of the hippocampal pyramidal cell, which may be due to the large difference in the location of the dendritic current injection. Resonance is an important property of linear electrical circuits as it can produce supralinear changes in impedance at the resonant frequency. For example, a resonant circuit can have a near-infinite impedance at the resonant frequency with a very low impedance at other frequencies.

Resonance and oscillations are common in the brain. Some of the earliest experiments on neuronal membrane noted preferences for certain frequencies (Cole & Curtis, 1939). Many types of neurons are known to fire periodically, and networks of neurons often show periodic activity (Llinás, 1988; Puil, Meiri, & Yarom, 1994). Until recently, experimental methods did not allow direct studies of dendrites, and their frequency response was thought to be governed by low-pass RC circuits (Rall, 1969; Tuckwell, Wan,

& Wong, 1984). Patch clamp studies have since enabled better observations of dendrites, which show that the dendritic membrane also has a frequency resonance (Ulrich, 2002; Cook, Guest et al., 2007; Hu et al., 2009; Narayanan & Johnston, 2007). Although many theories suggest how oscillatory effects, can arise from the structure of neurons, their voltage and time-dependent components or neural networks (Llinás, 1988; Pinsky & Rinzel, 1994; Mainen & Sejnowski, 1996; Hutcheon & Yarom, 2000), the role of the dendritic membrane in these oscillations is a fairly recent discovery.

Although resonance had been previously identified in somatic recordings (Hutcheon & Yarom, 2000; Puil et al., 1994), the implication of a resonance in Z_T is that dendrites have a bandpass feature that allows the resonant frequencies of the synaptic input to have a greater impact on somatic potentials. Experiments have also revealed that the H-channel is the primary voltage-dependent current that shapes the resonance property of Z_T (Ulrich, 2002; Cook, Guest et al., 2007; Hu et al., 2009; Narayanan & Johnston, 2007). However, computer models demonstrate that any arbitrary voltage-dependent conductance with the appropriate activation time constant can produce a similar resonance in Z_T (Hutcheon & Yarom, 2000; Cook, Willhelm et al., 2007).

The experiments illustrated in Figure 1 addressed transmission only between two points in the neuron. Thus, it is still an open question if the linear resonance property of Z_T shown in Figure 1 applies to all branches of the dendrite tree beyond the main trunk. However, given the robust experimental findings, it is important to understand the theoretical implications of linearity and resonance in a dendritic tree. Our goal was to combine the accuracy of the two-point transfer impedance with the realistic geometry of a reconstructed compartmental neuron model. We should note that transfer impedances have been used in compartmental models before (Carnevale & Johnston, 1982; Carnevale, Tsai, Claiborne, & Brown, 1997), but the application was restricted to passive dendrites. Specifically, we wanted to know how knowledge of Z_T could be combined with a compartmental model of a neuron to constrain the functional role of active dendrites.

3 Methods

We performed two types of computer simulations. In the first, we investigated if a published biophysically realistic CA1 hippocampal pyramidal neuron model would produce the same linear resonance signal transfer observed experimentally. This simulation was important to demonstrate that a model designed to reproduce the local synaptic nonlinearities would also capture the linear dendritic signal-transfer properties. The second set of simulations was more complex and focused only on the question of linear signal transfer in dendrites. In this case, we used the experimentally observed transfer impedance illustrated in Figure 1 to replace the

complex nonlinear channel models located in each compartment with a single membrane impedance function (Z_m).

3.1 Transfer Impedance of a Biophysically Realistic Pyramidal Neuron Model. In this first set of simulations, we tested the generality of the linear transfer impedance by simulating a nonlinear biophysically realistic model of a CA1 pyramidal neuron (Poirazi, Brannon, & Mel, 2003). This model is freely available from the NEURON repository and was originally published to produce nonlinear computations of synaptic inputs. For our simulation results in Figure 2, we adapted this model for continuous-time white-noise dendritic current injections to mimic the experimental paradigm of Figure 1 and then estimated the transfer impedance using standard linear regression.

3.2 Membrane Impedance Model of a Pyramidal Neuron. In our second set of simulations, we derived a linear impedance-based compartmental model of dendritic signal-transfer using the two-port analysis similar to Carnevale and Johnston (1982). The driving hypothesis of these simulations is that the complex voltage- and time-dependent channels that shape dendritic signal transfer can be modeled as linear impedances in the dendritic membrane (Z_m). We implemented compartmental models of two reconstructed cells: a hippocampal pyramidal neuron (Pyapali, Sik, Penttonen, Buzsaki, & Turner, 1998) and a cortical pyramidal neuron (Shepherd & Svoboda, 2005), both of which are publicly available through online databases. As the two models produced qualitatively similar results, we show only the CA1 results in Figures 4 and 5. A good reason for using a fully reconstructed model rather than a simplified model with a few compartments is that the transfer impedance (see Figure 1, Z_T) between two points in a cell is sensitive to the geometry of the entire neuron.

3.2.1 Two-Port Description of Transfer Impedance Z_T. For the simulations in Figures 4 and 5, we did not explicitly model nonlinear voltage- and time-dependent channels in the dendritic membrane. Instead, the unit membrane impedance $Z_m(f)$ was defined as a function of frequency and was specified in units of $\Omega \cdot \text{cm}^2$. The total membrane impedance $\hat{Z}_m$ in a cylindrical compartment is given by

$$\hat{Z}_m(f) = \frac{Z_m(f)}{\pi d l},$$

where d is the diameter of the compartment and l is the length. The axial resistance in a compartment was given by

$$\hat{R}_a = \frac{4R_a l}{\pi d^2}.$$

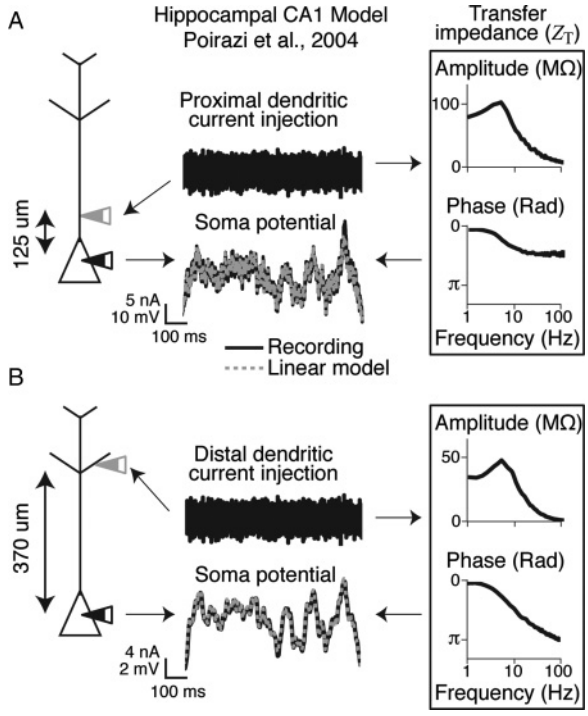

Figure 2: Linear transfer impedance (Z_T) accounts for the signal-transfer properties of a biophysically realistic neuron model. We adapted the detailed channel-based model (Poirazi et al., 2003) for continuous current injection to simulate the experiments in Figure 1. Although this model is capable of producing many kinds of nonlinearities, continuous-time current injection in the dendrites produced a linear dendrite-to-soma transfer impedance. (A) Proximal current injection at 125 μm. The linear model (gray dashed line) accounted for 97% of the variance in the soma potential (black trace). A bode plot of the linear model shown on the right demonstrates a band-pass resonance similar to experimental results. (B) Distal current injection at 370 μm. The linear model accounted for 97% of the dendrite-to-soma variance as well.

It is important to emphasize that $\hat{Z}_m$ depends on only frequency and is independent of other factors like signal amplitude.

When a signal travels through the neuron model, its voltage attenuation in a single compartment can be reduced to a multiplier (Carnevale et al., 1997). If we consider a voltage signal traveling toward the soma, the relationship between the amplitude at the distal end of the compartment V_1 and the voltage at the proximal end of the compartment V_0 is given by

$$V_0 = k_{in} \times V_1,$$

where k_{in} is the somatopetal attenuation term for the compartment. Likewise, for the relationship for a voltage signal traveling distally from the soma, the attenuation in a compartment is given by

$$V_1 = k_{out} \times V_0,$$

where k_{out} is the somatofugal attenuation term for the compartment. k_{in} and k_{out} are computed by a series of recursive passes, which are detailed elsewhere (Carnevale et al., 1997). We computed the input impedance Z_{input} at each end of the compartment using the same methods.

The transfer impedance Z_T between any two points in the model can be solved by isolating the path between the two points and using the attenuation and impedance terms. Consider a path with n segments, numbered 1 to n, where 1 is the most proximal compartment. The impedance between these two compartments is given by

$$Z_T = Z_{input,0}(1) \times \prod_{i=1}^{n} k_{out}(i),$$

where $Z_{input,0}(1)$ is the input impedance at the proximal end of the most proximal compartment in the path and the indices in parentheses specify the compartment number. The impedance between two points in a linear circuit is always symmetrical (Koch, 2004), so the same quantity can also be computed starting from the distal end. We used this method to compute transfer impedances, which we compared to experimental results.

We developed the model using Matlab r2011b. The axial resistance *Ra* was 150 $\Omega \cdot$ cm and based on previous estimates (Spruston, Jaffe, & Johnston, 1994). The membrane impedance, by comparison, was optimized using a parameter search.

3.2.2 Optimizing the Membrane Impedance Z_m. For the analysis shown in Figures 4 and 5, we performed a parameter search to find the membrane impedance (Z_m) that best produced the experimentally measured transfer impedance Z_T between the dendrites and soma. Figure 3B illustrates this analysis between dendritic compartment *a* and soma *s*. Before we could find the values of our membrane impedance, it was important to clearly define our parameter space.

We used three simplifications and assumptions to reduce the size of the parameter space to a single variable:

1. A linear model can be separated by frequency, and thus we were able to solve the transfer function value separately at each frequency.
2. We focused only on amplitude and neglected phase. An impedance is usually represented by a complex number, which can be separated

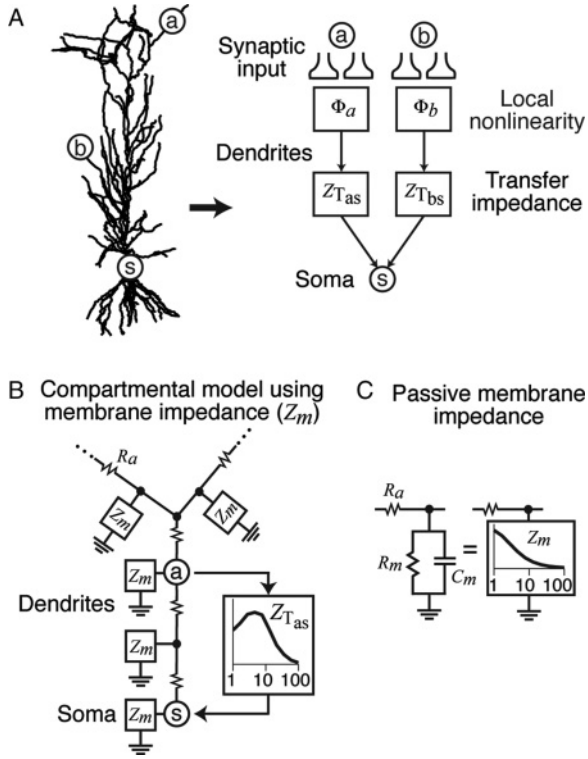

Figure 3: Transfer impedance (Z_T) and membrane impedance (Z_m) can be used to model dendritic signal transfer. Here, we illustrate how a linear model of dendritic signal transfer may fit into the larger picture of neuronal processing. This is an illustrative model, and in this study, we focused on only the linear transfer impedance. (A) The effect on the soma (s) from synaptic inputs at different dendritic locations (a and b) can be captured by local nonlinearities shaped by a transfer impedance (Z_T). One can extract Z_T to describe the electrical coupling between any two points in the model and is an extension of the two-point model in Figure 1. (B) Using a compartmental neuron model, we replaced the nonlinear voltage- and time-dependent channels with a membrane impedance (Z_m) in order to reproduce the experimentally observed transfer impedance (Z_{Tas}). Each compartment contained a membrane impedance Z_m and an axial resistance R_a. We did not include local nonlinearities in the models. (C) Example of the membrane impedance for a passive membrane compartment (phase is not shown).

into an amplitude component and a phase component. In this context, amplitude is related to the amount of attenuation, and phase is related to the delay a particular frequency experiences.

3. We applied one membrane transfer function throughout the dendritic tree. Although ion channel distributions differ along the dendrosomatic axis (Migliore & Shepherd, 2002), we used a single Z_m function for the entire cell.

The result of these assumptions is that there was only one free parameter per frequency. Finding the optimal value of our one-dimensional parameter space was accomplished by minimizing an error function,

$$\epsilon = (\hat{Z}_T(Z_m(f)) - Z_{\mathrm{T}}(f))^2,$$

where $\hat{Z}_T(f, Z_m)$ is the transfer impedance measured from the model for a particular frequency f and unit membrane impedance $Z_m(f)$. Z_{T} is an experimentally measured value as illustrated in Figure 3B.

Each frequency f was treated separately, and we tested Z_m values between $10^2\ \Omega \cdot \mathrm{cm}^2$ and $10^6\ \Omega \cdot \mathrm{cm}^2$. For each frequency, we selected the value of Z_m that minimized the error term ϵ.

4 Results

We used computer simulations to examine linear signal transfer in dendrites. We first asked if a biophysically realistic pyramidal neuron model designed to mimic nonlinear synaptic computations would also show a linear band pass transfer impedance similar to the experimental results in Figure 1. We next exploited this linearity to collapse the complex voltage- and time-dependent channel properties of a reconstructed neuron into a single uniform linear membrane impedance. Finally, we used this reduced model of the dendrite to explore the functional implications of two possible membrane impedance profiles.

4.1 Linear Signal Transfer in a Channel-Based Model. We first tested whether the signal-transfer properties of dendrites (illustrated in Figure 1) could be replicated in a nonlinear channel model of a CA1 pyramidal neuron. We adapted a model known for producing nonlinear summation of synaptic inputs (Poirazi et al., 2003) by injecting continuous white-noise current in the dendrites and estimating a linear transfer impedance Z_{T}. We found that under continuous current injection, this model robustly demonstrated linear behavior similar to the in vitro experiments (see Figure 2). We solved transfer impedances for two dendritic locations 125 μm and 370 μm from the soma. At 125 μm, the linear transfer function accounted for 97% of variance in the somatic membrane potential and Z_{T} showed resonance around 5 Hz (see Figure 2A). In this case, 0.7 % of the somatic response was discarded to remove action potentials. At a more distal dendritic location of 370 μm, the linear transfer function again accounted for 97% of variance, but no somatic action potentials occurred. Like the proximal case,

the distal Z_T showed resonance around 5 Hz (see Figure 2B). Thus, these simulations confirm previous modeling results (Hutcheon & Yarom, 2000; Cook, Willhelm et al., 2007) that illustrate nonlinear channels can produce linear transfer impedances under continuous-time input conditions.

4.2 A Functional Model of Linear Dendritic Signal Transfer. The notion that a linear impedance describes the signal-transfer properties from the dendrites to the soma fits with existing theories that dendrites also perform local nonlinear computations on synaptic inputs (Polsky et al., 2004; Larkum et al., 2009; Williams & Stuart, 2002; Gasparini et al., 2004). Our refinement of this illustrative model (see Figure 3A) is that local nonlinear processing of the synaptic input (ϕ) is further shaped by a linear transfer impedance (Z_T) before reaching the soma. For example, synaptic inputs at a in Figure 3A are combined by nonlinearities (ϕ_a), and the results of this computation are passed through the resonant transfer impedance (Z_{Tas}) before arriving at the soma (s).

Although the model in Figure 3A provides a description of signal transfer from any point in the dendrites to the soma, it does not tell us anything about the functional membrane properties of dendrites. In other words, if the dendrite-to-soma transfer impedance Z_T accounts for almost all of the signal transfer characteristics during a continuous-time input regime, then what can we conclude about the functional property of the dendritic membrane? Figure 3B illustrates this question in terms of a compartmental model where the voltage- and time-dependent channels are functionally expressed as a linear membrane impedance (Z_m). Note that Z_{Tas} in Figure 3B is the experimental transfer impedance measured in Figure 1A.

One possibility is that each box labeled Z_m in Figure 3B is in fact a nonlinear function, but together the collective network of nonlinearities in the dendrites produces a linear Z_{Tas} from dendritic location a to the soma (s). A far simpler assumption, which we explore here, is that under the continuous-input regime, each Z_m is also linear. Furthermore, this reduces the neuron to a more tractable model that can be easily solved. An example of Z_m for a passive RC membrane is shown in Figure 3C. However, it is obvious that no combination of passive Z_m would produce the experimentally measured resonance of Z_{Tas} illustrated in Figure 3B.

Before we present two potential solutions for Z_m, it is important to emphasize that Z_T is more than an abstract description of the neuron between two electrodes. A transfer impedance is an intuitive way to think about dendritic signal processing in terms of the frequency response and fits well with current models of dendritic processing that combine linear and nonlinear mechanisms.

4.3 Optimizing a Uniform Membrane Impedance. As illustrated in Figure 3B, we wanted to know what Z_m accounts for the experimentally observed Z_T? For this analysis, the voltage- and time-dependent channels

in a compartmental model of a neuron are replaced with a single membrane impedance. Note that we focused on the amplitude of Z_m and Z_T and ignored phase. Even assuming linearity, there still exists an infinite number of combinations of Z_m that would produce a given Z_T between two points in the model. Therefore, we had to make additional assumptions about the distribution of Z_m. Our first approach was to assume that the unit membrane impedance $Z_m(f)$ was uniform throughout the cell. We then optimized Z_m at each frequency to approximate the experimentally observed Z_T of our two example neurons from Figure 1. Because the results were qualitatively similar for the hippocampal and cortical pyramidal neurons, we present results only for the reconstructed CA1 model here (see Figure 4A).

To mimic the experimental recordings in Figure 1A, the soma-to-dendrite Z_T was measured in the model using the same distance between the dendrite and soma locations (see Figure 4A). We then optimized Z_m in the reconstructed model (see Figure 4B, bottom) to produce the same experimentally observed Z_T (Figure 4B, top), which has the same resonance near 5 Hz. Z_m had an aptitude of 14 k$\Omega \cdot$ cm^2 at 0 Hz and 22 k$\Omega \cdot$ cm^2 at 4.6 Hz, the resonant frequency. Using this optimized Z_m in our CA1 model reproduced the experimental transfer impedance (compare Z_T in Figures 4B, top, and Figure 1A). Thus, a single resonant membrane impedance distributed throughout the dendrites and soma accounted for the experimentally observed soma-to-dendrite transfer impedance.

Using the optimized uniform value of Z_m (see Figure 4B, bottom), we also measured the model's Z_T from different dendritic locations. There was a strong location dependence of the soma-to-dendrite Z_T such that the transfer impedance was reduced as a function of distance from the soma (see Figure 4C). One interesting aspect of the location dependence of Z_T was that it was minimized at the resonant frequency. This is shown in Figure 4D as the ratio of the transfer impedances at 150 μm and 650 μm from the soma (referred to as dendritic transfer). The peak in dendritic transfer at about 48% suggested that resonance in Z_m could be used to minimize the location-dependent variability of Z_T at the resonant frequency. We also found that resonance strength increased with distance, which agrees with experimental results (Narayanan & Johnston, 2007).

4.4 Optimizing Z_m to Reduce Location-Dependent Attenuation at the Resonant Frequency. One of our original goals in designing this model was to investigate the effect of attenuation on current signals that arrive in different parts of a neuron. The resonant property of dendrites may be a signature that dendrites are trying to minimize attenuation at the resonant frequency. Indeed, the resonant frequency of an electrical circuit corresponds to the frequency with the highest impedance. We next demonstrate an extreme case, which shows how the distribution of a uniform Z_m with a strong resonance can be used to minimize the dendrite-to-soma attenuation at the resonant frequency.

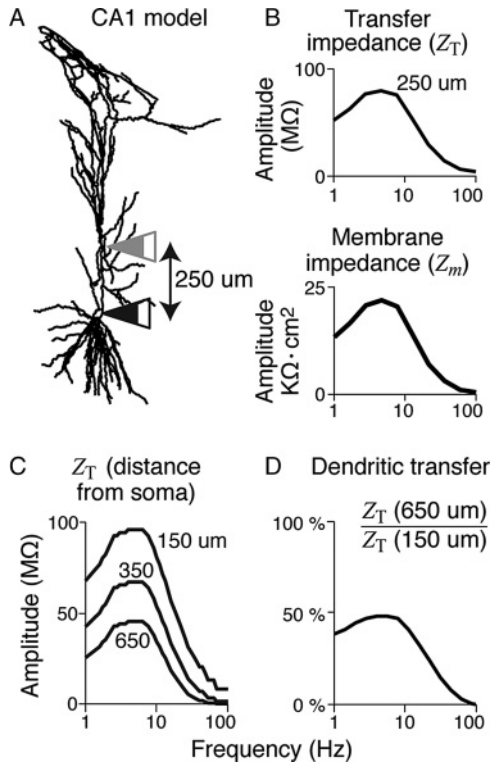

Figure 4: Optimizing a single membrane impedance (Z_m) to account for the experimentally observed transfer impedance (Z_T). (A) A reconstructed CA1 hippocampal neuron (Payapali et al., 1998) was used to construct a compartmental model using a uniform Z_m. The membrane impedance captured the net effect of the voltage- and time-dependent channels. In these simulations, we optimized Z_m to reproduce the transfer impedance between the soma and dendrites that corresponded with the 250 μm electrode separation in the CA1 experiment in Figure 1A. (B) Top: The transfer impedance of the model. Bottom: The optimized membrane impedance of all compartments that produced the transfer impedance. (C) Dendrite-to-soma transfer impedance at several distances from the soma using the optimized Z_m in panel B (bottom). More distal sites show a higher degree of attenuation and slightly stronger resonance. (D) Dendritic transfer quality. The ratio of the dendrite-to-soma transfer impedance at 650 μm and 150 μm. At the resonant frequency, the site at 650 μm produces somatic voltage deflections about 48% as large as the 150 μm site.

We created this scenario by placing a large conductance in the soma and then fitting the model to reproduce the same experimentally observed transfer impedance in Figure 1A. Figure 5A shows Z_T (left, which is the

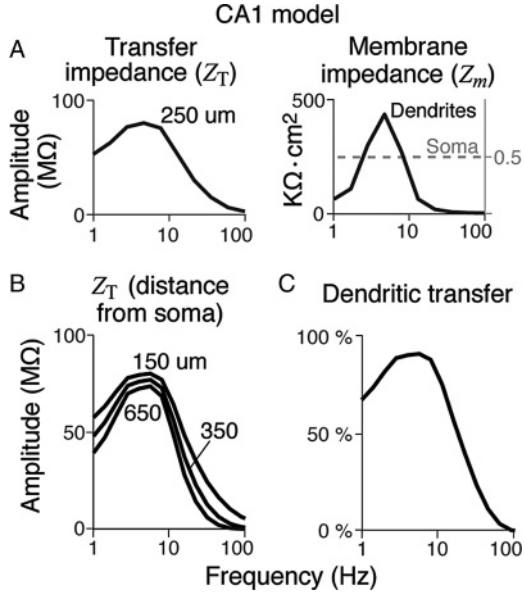

Figure 5: Resonance can minimize dendritic attenuation. We set the membrane conductance to 500 $\Omega \cdot \text{cm}^2$ in the soma and refit Z_m in the model illustrated in Figure 4A. Under these conditions, signals traveling from the dendrites to the soma experience very little attenuation at the resonant frequency. (A) Left: The dendrite-to-soma transfer impedance of the optimized model. Right: The membrane impedance of the soma (gray dashed line) and dendrites (black), which produced the desired transfer impedance. (B) Dendrite-to-soma transfer impedance at several distances from the soma. (C) The ratio of the transfer impedance at 650 μm to the transfer impedance at 150 μm. Near the resonant frequency, the 650 μm is coupled to the soma almost as strongly as the 150 μm point, with the ratio peaking at 92%.

same as Figure 4B) and Z_m (right) for the optimized CA1 model. Z_m had an amplitude of 62 $\text{k}\Omega \cdot \text{cm}^2$ at 0 Hz, and 430 $\text{k}\Omega \cdot \text{cm}^2$ at 4.6 Hz, the resonant frequency.

The large somatic conductance was necessary to reproduce the same transfer impedance by setting Z_m to 500 Ω/cm^2 in the soma compartment (dashed gray line, Figure 5A). This led to a relatively uniform voltage drop from the dendrites to soma, independent of dendrite location (see Figure 5B). This is especially prominent at the resonant frequency, where the location dependence of Z_T was nearly eliminated, with the dendritic transfer ratio improved to 92% (see Figure 5C). This version of the model also shows increased resonance in Z_T at distal dendritic points (see Figure 5B).

This and the previous model together illustrate the degree of variation in Z_m profiles that can produce the same dendrite-to-soma Z_T. Although the two models produced the same transfer impedance at 250 μm (compare Z_T in Figures 4B and 5A), the dendritic Z_m profiles are very different. In the first model, Z_m is similar to the Z_T, while in the second, Z_m has a much stronger resonance. Thus, a neuron's dendrite-to-soma transfer impedance is shaped by the relative membrane impedances throughout the soma and dendrites.

5 Discussion

Our functional model based on a linear membrane impedance (Z_m) captured the experimentally observed dendrite-to-soma transfer impedance (Z_T). We believe that this is a strong case for the value of the model, especially applied to a continuous-time input regime. Although the transfer impedance represents a satisfying functional model of dendritic signal processing, it does not constrain the underlying distribution of membrane impedances across the dendritic axis. Nevertheless, representing the collective effect of voltage-dependent ion channels as an impedance provides a powerful framework for understanding the contribution of the dendritic membrane in shaping the dendritic signal-transfer characteristics.

The scope of this model is limited in several ways. First, the model applies to continuous current injection only within a certain range of intensity. Sudden impulses of current to resting membrane can produce nonlinear responses, which would not be accounted for by the linear model. We believe that continuous current injection mimics the effects of simultaneous input from many synapses. Sufficiently large current injection can invoke dendritic spikes (Kandel, Spencer, & Brinley, 1961; Golding & Spruston, 1998), which are an inherently nonlinear phenomenon. In experiments, however, even when when the current injection was strong enough to produce realistic somatic spike rates in the soma, the linear-transfer impedance still accounted for most of the dendrite-to-soma input-output properties (Cook, Guest et al., 2007). Furthermore, the section of the apical trunk nearest to the soma has been suggested to be more excitable than the rest of the cell (Kandel et al., 1961; Polsky et al., 2004). Thus, if signal transfer near the soma is linear, it stands to reason than signal transfer in more distal regions would also be linear.

Experiments have shown that the effect of several simultaneous synaptic inputs on the soma can be greater than the linear sum of the individual inputs (Polsky et al., 2004; Larkum et al., 2009; Williams & Stuart, 2002; Gasparini et al., 2004). Within our linear model, these effects can be accounted for as local nonlinearities connected by linear transfer impedances (see Figure 3A). Reconciling the linearity observed under the continuous-time input regime with the nonlinearities observed under other input

regimes, however, is a challenge in developing a functional model of dendrites.

The resonance property of the transfer impedance could explain spontaneous theta oscillations and frequency-selective cells (Ulrich, 2002; Cook, Guest et al., 2007; Hu et al., 2009; Narayanan & Johnston, 2007). The shape of the transfer impedance is a low-pass filter with a resonant response in the theta band. This means that low-frequency signals generally have a larger effect on the soma, but that signals at a particular frequency in the theta band (the resonant frequency) have the largest effect (Hutcheon & Yarom, 2000). Cells in the hippocampus are known to preferentially fire at frequencies in the theta band (Buzsaki, 2002), and theta oscillations arise spontaneously in the soma and dendrites (Buzsaki, Kamondi, Acsady, & Wang, 1998) of cells. The most common explanation for this phenomenon is that the oscillations come from periodic signals from other brain areas (Buzsaki, 2002), but resonant cell membranes could produce theta oscillations from nonperiodic input patterns. In addition, resonance properties vary along the dendrosomatic axis (Narayanan & Johnston, 2007). Some of these variations, like the increase in resonance strength, arise naturally in our model. Others, like the variation in resonant frequency, would require a nonuniform distribution of Z_m.

Is synaptic location part of the neural code? The weak contribution to somatic membrane potential of any one synapse (Williams & Stuart, 2002; Nevian et al., 2007), together with the fact that input signals may be spatially distributed across the dendrites (Jia et al., 2010), could by default ameliorate the effects of synaptic location. Alternatively, if synaptic location is to be actively removed from the neural code, there are two ways that distal and proximal synapses could have similar effects on the soma. First, distal inputs could be amplified to counteract the effects of attenuation, which could be accomplished with higher synaptic conductance at distal synapses (Magee & Cook, 2000) or nonlinear effects (Williams & Stuart, 2002). Second, Efficient electrical conduction in dendrites could reduce attenuation (Cook & Johnston, 1997, 1999). If signals are efficiently conducted through the dendritic tree, then two synapses at different distances will have similar effects on the soma. Our simulations in Figures 4 and 5 suggest that resonance in the transfer impedance is a signature that dendrites are reducing the location-dependent attenuation of signals in the resonant-frequency band. This function of resonance is most appealing for a global sum-threshold model of a neuron that ignores the effect dendritic location has in the synaptic input, which is commonly used in computational and systems neuroscience (Shadlen & Newsome, 1994; Ferster & Spruston, 1995).

6 Conclusion

The strength of our model is its ability to account for experimental results using continuous-time inputs and that transfer impedances are intuitive and

predictable. The value at each frequency represents the size of a voltage deflection in response to a current. Unlike models with explicit voltage-dependent channels, where complex interactions between diverse channels determine the behavior, a single number characterizes the transfer function's behavior at each frequency. Furthermore, impedance models require very little computational power to simulate and are more computationally efficient than time-domain simulations (Carnevale et al., 1997). For this reason, they are useful for large-scale simulations of networks of reconstructed neurons.

References

Berger, T., Larkum, M. E., & Lüscher, H. R. (2001). High I(h) channel density in the distal apical dendrite of layer V pyramidal cells increases bidirectional attenuation of EPSPS. *Journal of Neurophysiology*, *85*(2), 855–868.

Buzsaki, G. (2002). Theta oscillations in the hippocampus. *Neuron*, *33*(3), 325–340.

Buzsaki, G., Kamondi, A., Acsady, L., & Wang, X. J. (1998). Theta oscillations in somata and dendrites of hippocampal pyramidal cells in vivo: Activity-dependent phase-precession of action potentials. *Hippocampus*, *8*(3), 244–261.

Carnevale, N. T., & Johnston, D. (1982). Electrophysiological characterization of remote chemical synapses. *J. Neurophysiol.*, *47*(4), 606–621. http://www.hubmed.org/fulltext.cgi?uids=7069456

Carnevale, N. T., Tsai, K. Y., Claiborne, B. J., & Brown, T. H. (1997). Comparative electrotonic analysis of three classes of rat hippocampal neurons. *Journal of Neurophysiology*, *78*(2), 703–720.

Cash, S., & Yuste, R. (1999). Linear summation of excitatory inputs by CA1 pyramidal neurons. *Neuron*, 22(2), 383–394.

Cole, K. S., & Curtis, H. J. (1939). Electric impedance of the squid giant axon during activity. *J. Gen Physiol.*, *22*(5), 649–670. http://www.hubmed.org/fulltext.cgi?uids=19873125

Cook, E. P., Guest, J., Liang, Y., Masse, N., & Colbert, C. (2007). Dendrite-to-soma input/output function of continuous time-varying signals in hippocampal CA1 pyramidal neurons. *J. Neurophysiol.*, *98*(5), 2943–2955.

Cook, E. P., & Johnston, D. (1997). Active dendrites reduce location-dependent variability of synaptic input trains. *Journal of Neurophysiology*, *78*(4), 2116–2128.

Cook, E. P., & Johnston, D. (1999). Voltage-dependent properties of dendrites that eliminate location-dependent variability of synaptic input. *Journal of Neurophysiology*, *81*(2), 535–543.

Cook, E. P., Willhelm, A. C., Guest, J. A., Liang, Y., Masse, N. Y., & Colbert, C. M. (2007). The neuronal transfer function: Contributions from voltage and time-dependent mechanisms. *Progress in Brain Research*, *165*, 1–12.

Ferster, D., & Spruston, N. (1995). Cracking the neuronal code. *Science*, *270*(5237), 756–757.

Gasparini, S., Migliore, M., & Magee, J. (2004). On the initiation and propagation of dendritic spikes in CA1 pyramidal neurons. *J. Neurosci.*, *24*(49), 11046–11056.

Golding, N. L., & Spruston, N. (1998). Dendritic sodium spikes are variable triggers of axonal action potentials in hippocampal CA1 pyramidal neurons. *Neuron*, *21*(5), 1189–1200. http://www.hubmed.org/fulltext.cgi?uids=9856473

Hu, H., Vervaeke, K., Graham, L. J., & Storm, J. F. (2009). Complementary theta resonance filtering by two spatially segregated mechanisms in CA1 hippocampal pyramidal neurons. *Journal of Neuroscience*, *29*(46), 14472–14483.

Hutcheon, B., & Yarom, Y. (2000). Resonance, oscillation and the intrinsic frequency preferences of neurons. *Trends in Neurosciences*, *23*(5), 216–222.

Jia, H., Rochefort, N., Chen, X., & Konnerth, A. (2010). Dendritic organization of sensory input to cortical neurons in vivo. *Nature*, *464*(7293), 1307–1312.

Kandel, E. R., Spencer, W. A., & Brinley, F. (1961). Electrophysiology of hippocampal neurons i. sequential invasion and synaptic organization. *Journal of Neurophysiology*, *24*, 225–242.

Koch, C. (2004). *Biophysics of computation: Information processing in single neurons*. New York: Oxford University Press.

Larkum, M. E., Nevian, T., Sandler, M., Polsky, A., & Schiller, J. (2009). Synaptic integration in tuft dendrites of layer 5 pyramidal neurons: A new unifying principle. *Science*, *325*(5941), 756–760.

Llinás, R. R. (1988). The intrinsic electrophysiological properties of mammalian neurons: Insights into central nervous system function. *Science*, *242*(4886), 1654–1664. http://www.hubmed.org/fulltext.cgi?uids=3059497

Magee, J. C., & Cook, E. P. (2000). Somatic EPSP amplitude is independent of synapse location in hippocampal pyramidal neurons. *Nature Neuroscience*, *3*(9), 895–903.

Mainen, Z. F., & Sejnowski, T. J. (1996). Influence of dendritic structure on firing pattern in model neocortical neurons. *Nature*, *382*(6589), 363–366. http://www.hubmed.org/fulltext.cgi?uids=8684467

Migliore, M., & Shepherd, G. (2002). Emerging rules for the distributions of active dendritic conductances. *Nature Reviews Neuroscience*, *3*(5), 362–370.

Morel, D., & Levy, W. (2009). The cost of linearization. *J. Comput. Neurosci.*, *27*(2), 259–275. http://www.hubmed.org/fulltext.cgi?uids=19343490

Narayanan, R., & Johnston, D. (2007). Long-term potentiation in rat hippocampal neurons is accompanied by spatially widespread changes in intrinsic oscillatory dynamics and excitability. *Neuron*, *56*(6), 1061–1075.

Nevian, T., Larkum, M., Polsky, A., & Schiller, J. (2007). Properties of basal dendrites of layer 5 pyramidal neurons: A direct patch-clamp recording study. *Nature Neuroscience*, *10*, 206–214.

Pinsky, P. F., & Rinzel, J. (1994). Intrinsic and network rhythmogenesis in a reduced Traub model for CA3 neurons. *J. Comput. Neurosci.*, *1*(1–2), 39–60. http://www.hubmed.org/fulltext.cgi?uids=8792224

Poirazi, P., Brannon, T., & Mel, B. (2003). Arithmetic of subthreshold synaptic summation in a model CA1 pyramidal cell. *Neuron*, *37*(6), 977–987.

Polsky, A., Mel, B. W., & Schiller, J. (2004). Computational subunits in thin dendrites of pyramidal cells. *Nature Neuroscience*, *7*(6), 621–627.

Puil, E., Meiri, H., & Yarom, Y. (1994). Resonant behavior and frequency preferences of thalamic neurons. *J. Neurophysiol.*, *71*(2), 575–582. http://www.hubmed.org/fulltext.cgi?uids=8176426

Pyapali, G. K., Sik, A., Penttonen, M., Buzsaki, G., & Turner, D. A. (1998). Dendritic properties of hippocampal CA1 pyramidal neurons in the rat: Intracellular staining in vivo and in vitro. *J. Comp. Neurol.*, *391*(3), 335–352. http://www.hubmed.org/fulltext.cgi?uids=9492204

Rall, W. (1969). Time constants and electrotonic length of membrane cylinders and neurons. *Biophys. J.*, *9*(12), 1483–1508. http://www.hubmed.org/fulltext.cgi?uids=5352228

Shadlen, M. N., & Newsome, W. T. (1994). Noise, neural codes and cortical organization. *Current Opinion in Neurobiology*, *4*(4), 569–579.

Shepherd, G. M., & Svoboda, K. (2005). Laminar and columnar organization of ascending excitatory projections to layer 2/3 pyramidal neurons in rat barrel cortex. *J. Neurosci.*, *25*(24), 5670–5679. http://www.hubmed.org/fulltext.cgi?uids=15958733

Spruston, N. (2008). Pyramidal neurons: Dendritic structure and synaptic integration. *Nature Reviews Neuroscience*, *9*(3), 206–221.

Spruston, N., Jaffe, D. B., & Johnston, D. (1994). Dendritic attenuation of synaptic potentials and currents: The role of passive membrane-properties. *Trends in Neurosciences*, *17*(4), 161–166.

Tuckwell, H. C., Wan, F. Y., & Wong, Y. S. (1984). The interspike interval of a cable model neuron with white noise input. *Biol. Cybern.*, *49*(3), 155–167. http://www.hubmed.org/fulltext.cgi?uids=6704439

Ulrich, D. (2002). Dendritic resonance in rat neocortical pyramidal cells. *Journal of Neurophysiology*, *87*(6), 2753–2759.

Williams, S., & Stuart, G. (2002). Dependence of EPSP efficacy on synapse location in neocortical pyramidal neurons. *Science*, *295*(5561), 1907–1910.

Received October 29, 2011; accepted June 17, 2012.